Separation Science and Technology
Publication details, including instructions for authors and subscription information:
http://www.informaworld.com/smpp/title~content=t713708471

Preparation and Evaluation of Fullers Earth Beads for Removal of Cesium from Waste Streams

Shameem Hasan[a]; Tushar K. Ghosh[a]; Dabir S. Viswanath[a]; Sudarshan K. Loyalka[a]; Bhaskar Sengupta[b]
[a] Nuclear Science & Engineering Institute and Particulate Systems Research Center, University of Missouri-Columbia, Columbia, Missouri [b] School of Chemical Engineering, Queens' University Belfast, Northern Ireland, UK

To cite this Article Hasan, Shameem , Ghosh, Tushar K. , Viswanath, Dabir S. , Loyalka, Sudarshan K. and Sengupta, Bhaskar(2007) 'Preparation and Evaluation of Fullers Earth Beads for Removal of Cesium from Waste Streams', Separation Science and Technology, 42: 4, 717 — 738
To link to this Article: DOI: 10.1080/01496390601173952
URL: http://dx.doi.org/10.1080/01496390601173952

Separation Science and Technology, 42: 717–738, 2007

ISSN 0149-6395 print/1520-5754 online
DOI: 10.1080/01496390601173952

Preparation and Evaluation of Fullers Earth Beads for Removal of Cesium from Waste Streams

Shameem Hasan, Tushar K. Ghosh, Dabir S. Viswanath, and Sudarshan K. Loyalka
Nuclear Science & Engineering Institute and Particulate Systems Research Center, University of Missouri-Columbia, Columbia, Missouri

Bhaskar Sengupta
School of Chemical Engineering, Queens' University Belfast, Northern Ireland, UK

Abstract: Fullers earth beads and cylinders were prepared using chitosan and sodium silicate as binders, respectively, for removal of cesium ion from aqueous solutions. The cost of the adsorbent is expected to be significantly lower as the raw materials are low cost materials and readily available. The adsorbents were characterized by SEM, EDS, and x-ray microanalysis. Adsorption capacity of the beads was evaluated under both batch and dynamic conditions. The adsorption capacity for Fullers earth beads was found to be 26.3 mg/g of adsorbent at 293 K when the liquid phase concentration of cesium was 1000 mg/L. The adsorption capacity of Fullers earth cylinder was found to be higher than that of beads, however, it was concluded that the alkaline nature of the cylinder precipitated out cesium increasing its capacity. The capacity of Fullers earth beads decreased by almost 62% when 1 mol/L NaCl and 2.25 mmol/L of strontium were present in the solution. The Freundlich, the Langmuir isotherm equations, and a modified Polanyi's equation were used to correlate the data. The isosteric heats of adsorption suggested the heterogeneity of the surface and multilayer coverage. The first order reversible kinetic model adequately described the dynamic

Received 17 January 2006, Accepted 6 November 2006
Address correspondence to Tushar K. Ghosh, Nuclear Science & Engineering Institute and Particulate Systems Research Center, University of Missouri-Columbia, Columbia, Missouri 65211. Tel.: 1-573-882-9736; Fax: 1-573-884-4801; E-mail: ghosht@missouri.edu

system during the adsorption process. The adsorption (k_1) and desorption (k_2) rate constants were evaluated from the dynamic model.

Keywords: Chitosan, fullers earth, cesium, adsorption, regeneration

INTRODUCTION

Hundreds of storage tanks across the United States contain radioactive wastes that need to be remedied. The major radionuclides present in the tank are Cs-137 and Sr-89. The composition of these wastes is rather complex. Some of these wastes contain either high concentrations of sodium nitrate or sodium hydroxide, which could be disposed of as low level wastes if the radioactivity is reduced below the concentration level set by the US Nuclear Regulatory Commission (NRC) as described in 10CFR Part 61.

Chemical precipitation, evaporation, and ion exchange processes are generally used for the removal of Cs-137 and Sr-89 from the low and intermediate level waste solutions before discharging them into the environment (1). Lateef et al. (2) provided a review of various methods including solvent extraction, liquid membrane separation, and ion exchange process for extraction of cesium and strontium from waste solutions. Among these methods, the ion exchange appeared to be the most effective in controlling radioactive wastes. In an attempt to find a suitable ion exchange resins for the removal of cesium and strontium from waste solution, several investigators have tried a number of inorganic, organic, and bio-adsorbents, with a varying degree of success (3–6). Dozol et al. (5) provided a review of various methods for removal of cesium from waste streams. They concluded that calix[4]arenas could be a very good material for removal of cesium from both acidic and alkaline solutions. Instability to radiation and highly basic nature of the solution cause decomposition of these adsorbents to undesirable, hazardous byproducts making these adsorbents unsuitable for removal of radionuclides (7).

Sing and Misra (8) reported that inorganic resin metal, hexacyanoferrate, can be used as a highly selective ion exchange resin for the removal of cesium from a variety of salt and acidic solutions. A similar observation was made by Harjula et al. (9) However, the cost of metal cyanoferrate for use on an industrial scale was found to be too high (8). Anthony et al. (10) developed a crystalline silicotitanate (CST) for removal of radioactive cesium from aqueous nuclear wastes. Zheng et al. (7) reported that CST is stable to radiation, highly selective for cesium relative to sodium, potassium, rubidium, and protons, and performs well in acidic, neutral, and basic solutions. Lee et al. (11) investigated a number of ion exchange resins using actual liquid wastes from the Department of Energy (DOE) storage sites. The sorbents initially tested included resorcinol formaldehyde resin (RF), CS-100 resin, Superlig 644C resin, granular potassium cobalt hexacyanoferrate, and granular crystalline silicotitanate (CSTs). Their study indicated that CST materials performed better than any of the other

materials under the experimental conditions tested in the laboratory. The adsorption capacity of various materials for cesium is summarized in Table 1. As can be seen from the table, the distribution coefficient (K_d) varied from 13 to 100,000 mL/g. However, the results using CST or other adsorbents from a field test are not available, and also the cost of these adsorbents could be a major factor for treatment of these wastes. Therefore, development of a low cost adsorbent is highly desirable.

In this work we prepared Fullers earth beads using chitosan as a binder and Fullers earth cylinder using traditional sodium silicate binder. Fullers earth is a low cost material that occurs naturally. However, Fullers earths in its natural form, even the granules, are very soft and are crushed easily making it unsuitable for use in an adsorption column. Chitosan is found to be an excellent adsorbent for a number of heavy metals including Cr, Cd, Cu, and As (12). Interestingly, chitosan was found to have negligible adsorption capacity for Cs. Therefore, the role of chitosan here is only as a binder. Adsorption capacity of Fullers earth based adsorbents for Cs was evaluated under both batch and dynamic conditions. The equilibrium adsorption data

Table 1. Adsorption of cesium on different adsorbent materials

Adsorbents	Concentration of Na^+ in the solution (mol/L)	K_d (mL/g) for cesium adsorption	References
Hydrous crystalline sodium silicotitanate	5.1 ($NaNO_3$)	900–1000	(3)
Hydrous crystalline silicotitanate	5.7	150–100,000	(7)
Chabazite	4.9	N/A	(24)
Clinoptilolite	4.99	7	(25)
Bauxite	4.99	65	(26)
Bentonite	4.99	1200	(27)
Chabazite (Na-modified)	14.3 (mg/L)	80000	(28)
Montmorillonite	5	36	(29)
Sodium titanate	4.99	13	(25)
Hydrous crystalline sodium silicotitanate	5.1	10000	(10)
Pharmacosiderites (KtiGe)	5	19	(25)
Potassium titanosilicate (KtiSi gel)	5	52	(25)
Sodium nonatitanate (NaTi)	5	13	(25)
Fe(II) hexacyanocobaltate (III)	1M HNO_3	9800	(1)
Resorcinol formaldehyde resin	1	19260	(30)
Fullers earth bead	1	110	Present work
Fullers earth bead[a]	1	400	Present work

[a]Based on Fullers earth only (chitosan free basis).

were correlated using the Freundlich, the Langmuir isotherm equations, and a modified Polanyi's potential theory (13).

EXPERIMENTAL

Materials

Fullers earth, which mainly contains calcium and magnesium silicate, was obtained from Fisher Scientific Co., NJ, USA. Fullers earth adsorbent was prepared both as spherical beads using chitosan as a binder and as small cylinders using traditional sodium silicate (14% NaOH, and 27% SiO_2, 59% H_2O) solution as a binder.

Preparation of Chitosan Coated Beads

Fullers earth powder of 35 mesh was first soaked with 0.2 mol/L oxalic acid for 4 h. This helped to introduce various functional groups onto Fullers earth, which in turn helped adhesion of chitosan onto Fullers earth later during the bead making process. Following this, it was washed with distilled water and dried in an oven for 12 h. Although washing with distilled water was not necessary, it was done to maintain a desired ratio of oxalic acid to chitosan which was found to be important for the performance of beads as adsorbent. Higher concentration of oxalic acid will require a greater concentration of NaOH and a greater amount of water during the bead making process. 60 g of acid washed Fullers earth was mixed with 30 g of chitosan flakes in a beaker with 1L, 0.2 mol/L oxalic acid. The mixture was stirred for 4 h while heating at 313–323 K (40–50°C) to obtain a homogeneous mixture. The spherical beads of Fullers earth were prepared by drop-wise addition of the mixture into a 0.7 mol/L NaOH precipitation bath. The beads were washed with deionized water to a neutral pH and freeze dried for subsequent use. A detailed description of the bead preparation method is discussed by Hasan et al. (14).

When sodium silicate was used as a binder, 10 gram of Fullers earth powder was mixed with 200 mL of 20 wt (%) of sodium silicate binder. The mixture was then passed through an extruder to make cylinder as it cannot be processed to make beads in the same manner as was done for chitosan-binder. These cylinders were heated at 70°C for 12 h in a vacuum oven. The dried cylinders were further cut into small pieces and heated at 400°C in a furnace for another 12 h. It was then washed thoroughly by deionized water to remove remaining sodium silicate from the surface. However, all of the sodium silicate could not be removed even after washing 8 times using a total of 3 L water. It had a significant effect on the adsorption capacity and has been discussed later. Finally, the cylinders were dried at 70°C in vacuum oven and were ready for further use.

Experimental Procedure

Equilibrium batch adsorption studies were carried out by exposing the beads to aqueous solutions of cesium of different concentrations in 125 mL Erlenmeyer flasks to a pre-determined temperature. About 0.25 g beads were added to 100 mL of solution. This amount of beads and solution assured that an equilibrium condition was reached, i.e., all of the cesium was not adsorbed by the beads, which would have made it difficult to determine the equilibrium point. The pH of the solutions was adjusted by adding either 0.1 mol/L hydrochloric acid or 0.1 mol/L sodium hydroxide. The flasks were placed in a constant temperature shaker bath for a specific time period. Following the exposure of beads to cesium, the samples were collected at predetermined time intervals. The solutions were filtered and the filtrates were analyzed for cesium by an Atomic Absorption Spectrometer. The adsorption isotherm at a particular temperature was obtained by varying the initial concentration of cesium ions. The amount of cesium adsorbed per unit mass of adsorbent (Q_e) was calculated using the following equation:

$$Q_e = \frac{(C_i - C_e)V}{M} \tag{1}$$

RESULTS AND DISCUSSION

Characterization of the Beads

The physical properties of the beads are given in Table 2. The amount of chitosan present in the beads was determined by a thermogravimetric analyzer by heating the beads at a rate of 10°C/min up to a temperature of 800°C in the presence of air. Chitosan started to burn out at 200°C and a

Table 2. Physical properties of Fullers earth based adsorbents

	Adsorbents	
Properties	Fullers earth beads	Fullers earth cylinders
Particle diameter, d_p (m)	2.2×10^{-3}	1.8×10^{-3} m (dia) and 1 cm long
Particle density, ρ (kg/m^3)	272	–
Particle porosity, ε_p	2.2×10^{-3}	–
Shape	Spherical	Cylindrical
Chitosan content, (wt%)	32	–
Surface area, (m^2/g)	48.5	1.59
Pore volume, (m^3/kg)	1.03×10^{-4}	4.7×10^{-6}
Average pore diameter, (m)	8.26×10^{-9}	1.08×10^{-7}

complete burn out occurred around 500°C. It was found that 32% of the chitosan was present on Fullers earth. The surface area, pore volume, and the pore diameter were evaluated by nitrogen adsorption/desorption at 77 K using a Micromeritics ASAP 2010 surface analyzer. The adsorbents were outgassed at 378 K under a vacuum of <10 μmHg for a minimum period of 24 h.The Fullers earth adsorbent was further investigated by scanning electron microscopy (SEM) and Energy dispersive (EDS) x-ray microanalysis. The SEM micrographs of these adsorbents are shown in Fig. 1a and 1b. The SEM micrographs were taken using backscatter electrons with an accelerating potential of 20 keV. The SEM micrograph of the outer surface of Fullers earth beads shown in Fig. 1a appears to be porous in nature. The texture of cylindrical shaped Fullers earth adsorbent was significantly different from that of Fullers earth beads (Fig. 1b) due mainly to the presence of sodium silicate binder. The surface morphology of the adsorbents following adsorption of cesium also changed significantly as can be seen from Fig. 2a and 2b. Both the adsorbents became lumped after the adsorption of cesium. This may be due to the complex formation of cesium with the adsorbent.

The EDS x-ray microanalysis of the center of the bead after exposure to cesium solution is shown in Fig. 3. This suggests that cesium could diffuse to the interior of the bead and chitosan did not block the diffusion process. The characteristic peak for cesium is observed at 4.3 keV. There are also peaks at 1.05, 1.478, and 1.41 keV that were characteristics of Kα peak for sodium, aluminum and magnesium, respectively that are constituents of Fullers earth (15).

The BET (Brunauer-Emmett-Teller) surface area of chitosan, Fullers earth, Fullers earth beads, and Fullers earth cylinders was found to be 1.36, 103.4, 48.5, and 1.59 m^2/g, respectively. It appears that chitosan blocked a number of pores in Fullers earth, and the chitosan film was not porous enough to retain the original porosity of Fullers earth. The drop of surface area was significant in the case of Fullers earth cylinder since sodium silicate formed a nonporous coating on Fullers earth. The pore size distribution of Fullers earth beads and Fullers earth cylinders is shown in Fig. 4. The average diameter of the pores in Fullers earth beads and Fullers earth cylinders is 0.02 μm to 0.15 μm, respectively. There are few pores in the 0.38 μm diameter range. The pore volume of Fullers earth beads was significantly greater than Fullers earth cylinders. It was 0.103 cm^3/g for the beads, whereas it was 0.0047 cm^3/g for the cylinders. It appears that chitosan or sodium silicate did not block the larger pores. As discussed further, larger pores may be responsible for the adsorption of cesium and there may be an optimum pore diameter for the adsorption of cesium. Although the surface area and pore volume of Fullers earth beads are significantly lower than other adsorbents such as activated carbon, chabazite, and montmorillonite, the adsorption capacity of Fullers earth beads or cylinders is comparable with them. It may be noted that the high surface area of activated carbon or other materials is due to the presence of micropores, which appears to be ineffective for adsorption of cesium. Therefore, it is not surprising that activated carbon has very low capacity for cesium.

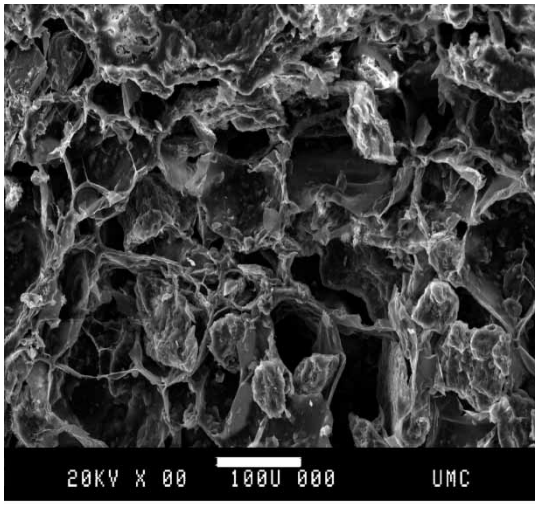

a)

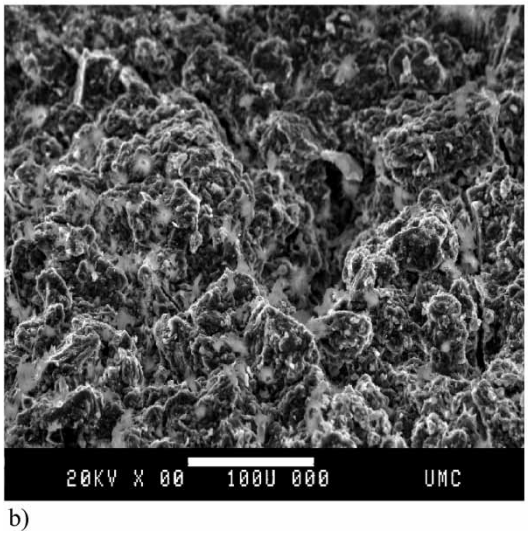

b)

Figure 1. Scanning electron micrograph of a) Fullers earth beads prepared using chitosan as a binder, b) Fuller's earth cylinder prepared using sodium silicate as a binder.

Effect of pH on Cesium Uptake

The effect of pH on adsorption of Cs by Fullers earth beads and cylinders is shown in Fig. 5. In these experiments, the initial pH of Cs containing solution was adjusted to the desired value using either HCl or NaOH

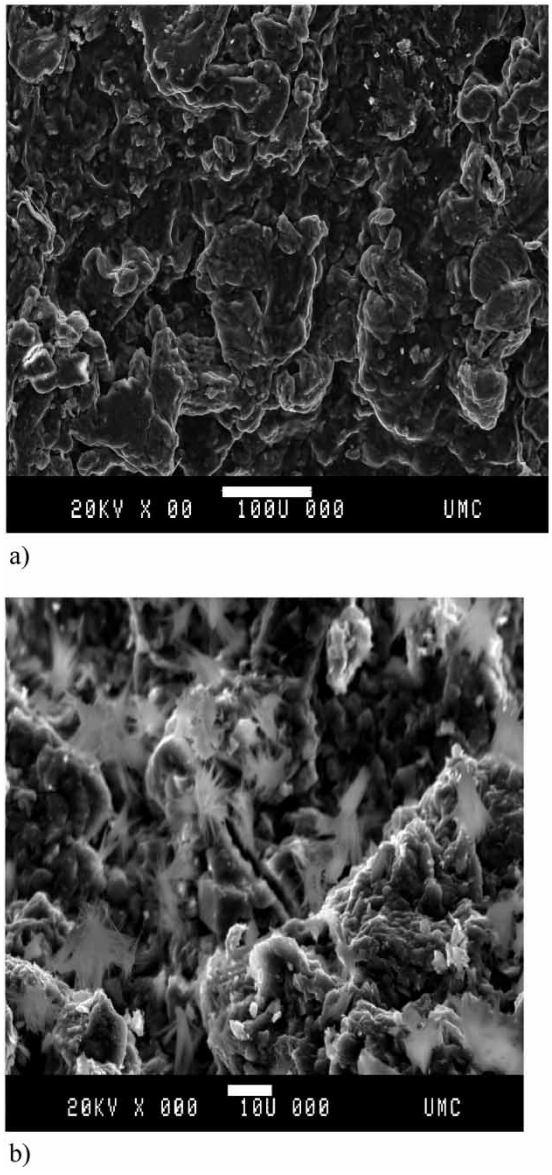

Figure 2. Scanning electron micrograph of; a) Fuller's earth beads and b) Fullers earth cylinders following exposure to CsCl solution.

solution. To the pH adjusted cesium solution, adsorbents were added. No attempt was made to maintain a constant pH of the solution using a buffer solution. It was noted that at the end of 24 h exposures, the pH of all the solutions increased, but the final pH of solutions exposed to Fullers earth

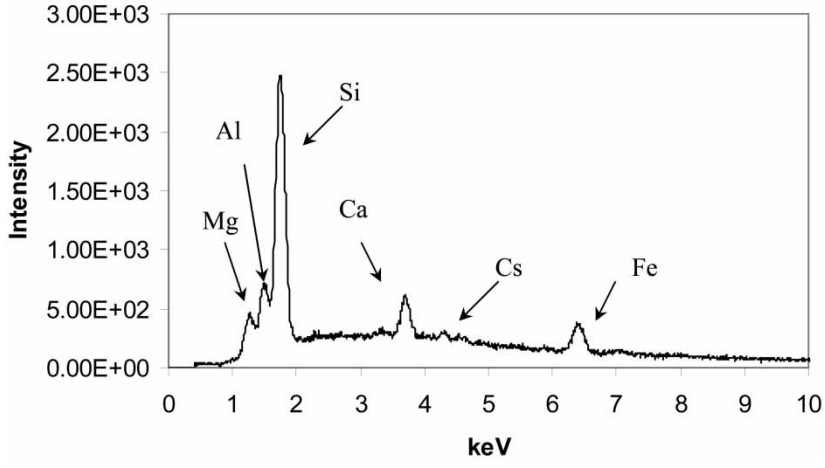

Figure 3. EDS x-ray microanalysis of Fullers earth beads exposed to cesium chloride solution (concentration of cesium: 1.5 mmol/L; temperature: 303 K).

cylinder was much higher compared to when beads were used. The final pH of solutions when cylinder was used were in the range of 11.5 to 12.0. The adsorption of cesium ion should result in a release of H^+ ion. This should normally reduce the pH of the solution. However, Kaminski and Modrzejewska (16) noted that the exchange of released H^+ ions occurs between the surface of the beads and solution resulting in the increase of pH of the

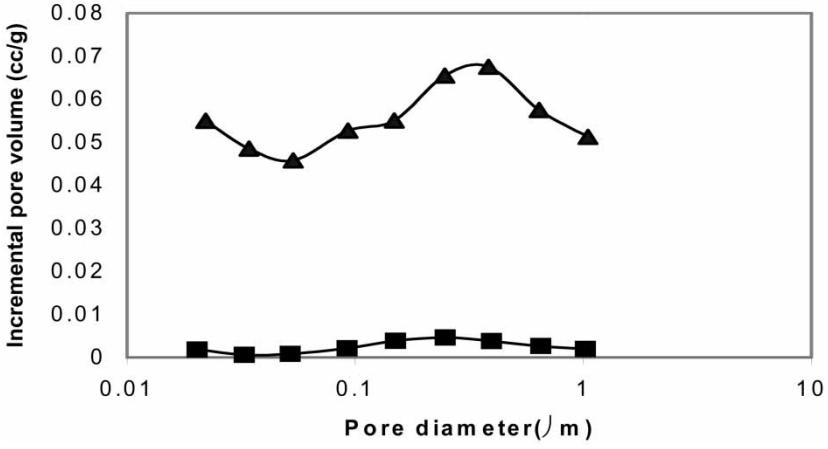

Figure 4. Incremental pore volume versus pore diameter of unexposed (■) Fullers earth cylinders, and (▲) Fullers earth beads.

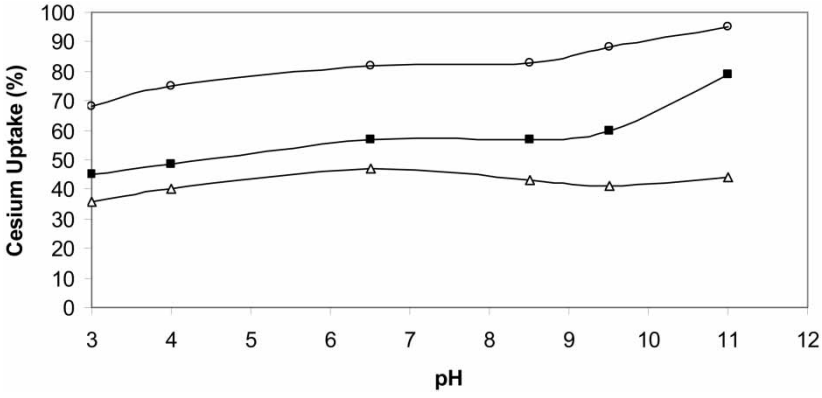

Figure 5. Effect of pH on cesium adsorption by (○) Fuller earth cylinder, (■) Fullers earth, (△) Fullers earth beads. (Initial cesium concentration: 1 mmol/L).

solution. A similar phenomenon should be also expected for cesium adsorption resulting in a higher pH of the final solution. Interestingly, Fullers earth cylinders showed a greater capacity for cesium than the beads even though cylinders had much lower pore volume. The adsorption of cesium increased on both adsorbents with the increase of pH of the aqueous solution up to a value of 6.5. The adsorption capacity started decreasing for beads at higher pH, but kept on increasing for cylinders at higher pH and at a faster rate above a pH of 9.0. The maximum uptake of cesium from aqueous solution was observed on Fullers earth cylinders at a pH 11. At pH higher than 7, cesium could undergo a reaction with hydroxyl ion in the solution and precipitate out. It may be assumed that Fullers earth cylinders that were prepared using sodium silicate as a binder might have helped surface precipitation of cesium due to the alkaline nature of the cylinders. As noted earlier, while preparing cylinders using sodium silicate as a binder, sodium silicate could not be removed from the cylinders even after several washes. The remaining sodium silicate increased the pH of the solution making it alkaline. The greater increase of pH of the solution in the presence of the cylinder-adsorbent seems to support this hypothesis. From the pH studies, it appears that Cs was mainly physiadsorbed on beads making it possible to regenerate and use repeatedly. Removal of cesium by precipitating it out of the solution was not the objective of this study. Therefore, Fullers earth cylinders were not further evaluated in this study. Although Fig. 5 shows that pure Fullers earth has a higher capacity than Fullers earth beads, it should be noted that the bead contained only 68% Fullers earth and the rest was chitosan binder. In our present study, since pure chitosan did not adsorb any cesium, the adsorption capacity on the basis of Fullers earth only should be 32% higher than that shown in Fig. 5. The present capacity is in the same range as other natural adsorbents such as chabazite and

montmorillonite. However, it is lower than synthetic silicotitanate based adsorbents. Although we have not done any direct cost comparison, the present adsorbent could be economical as all the raw materials are cheap and readily available. It also requires minimal processing compared to the preparation of silicotitanate based adsorbents.

XPS Analysis of Cesium Adsorbed onto Fullers Earth Beads

Figure 6 shows the binding energies of various components with Fullers earth as noted during XPS analysis. Peaks were obtained at binding energies 283, 398, 530.5, 101, 73, and 723.5 eV that correspond to C-1s, N-1s, O-1s, Si-2p, Al-2p, and Cs-3d, respectively. The XPS spectrum (Fig. 6) of the exposed bead also showed the presence of Cs-3d and Cs-4d peaks. The Cs-3d peaks showed two peaks; around 725.9 eV (Cs-3d5/2) and 736.5 eV (Cs-3d31/2). Cs-3d photoelectrons consist of Cs-3d5/2 and Cs-3d1/2 peaks that are the core level electrons and came essentially from the outer surface, while Cs-4d electrons originate from the inner core of beads (17).

Table 3 shows the Cs-3d5/2 binding energy with other elements. It may be concluded, based on the data given in Table 3 and Fig. 6, that cesium was present in the Fullers earth bead mainly as Cs^+ and a small amount as CsOH.

Adsorption Isotherms of Cesium on Fullers Earth Beads

The equilibrium adsorption isotherms of cesium on Fullers earth beads were determined at three temperatures—293, 303, and 313 K in the concentration

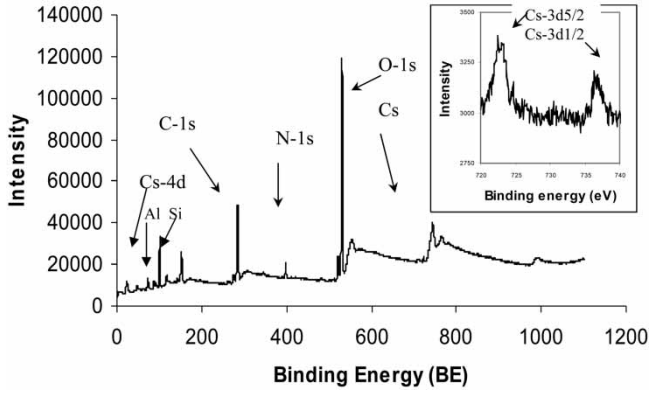

Figure 6. XPS spectrum of Fullers earth beads exposed to cesium chloride. Expanded view of XPS spectrum for cesium portion.

range of 0.38 mmol/L to 7.52 mmol/L and the equilibrium adsorption data are given in Table 4. As mentioned in the previous section, the maximum adsorption capacity of cesium on these beads occurred at a pH of 6.5. Therefore, the equilibrium isotherms experiments were carried out at a pH of 6.5, if not stated otherwise. The concentration profiles during cesium uptake by the beads from various concentrations of the solution are shown in Fig. 7. Almost 60% of cesium was adsorbed during the first 240 min of a run, and then the equilibrium was attained monotonically at 360 min in most of the runs. The adsorption isotherm data obtained at pH 6.5 showed Type I behavior. This suggests a monolayer adsorption of cesium on the bead. However, as discussed later, the heat of adsorption data indicated that the adsorbent is heterogeneous in nature. Therefore, the equilibrium adsorption data were correlated using both the Langmuir and the Freundlich isotherm equations. As can be seen from Table 4, the Langmuir equation provided the best fit of the data. The maximum absolute error was $\pm 5\%$ when the Langmuir equation was used. The values of the constants for both the Freundlich and Langmuir equations at various temperatures are listed in Table 4. Although the adsorbent was heterogeneous in nature as indicated by the heats of adsorption, the shape of the curve was Type I and the mathematical form of the Langmuir equation is best suited for this type of curve. Also, it is possible that the adsorbent had not reached saturation capacity. The multi-layer adsorption characteristics are more pronounced at the higher concentration or near the saturation capacity.

Effect of Cations on Cesium Uptake by Fullers Earth Beads

Sodium, strontium, and chloride are major ions present in great quantities in most of the radioactive waste tanks. Therefore, it will be more economical if any removal of cesium could be accomplished in the presence of these ions. The uptake of cesium was further investigated in the presence of NaCl in the concentration range of 0 to 1 mol/L and strontium concentration of 2.25 mmol/L. The uptake of cesium is found to decrease with the increase of NaCl concentration in the solution. When NaCl concentration was

Table 3. Absolute binding energy of different cesium compounds

Sample	Cs3d5/2 (eV)	References
Cs	724.5	(14)
Cs-H	725.1	(25)
CsOH	725.0	(25)
CsCl	723.8	(25)
Cs-Fullers earth beads	725.98	Present work

Table 4. Cesium uptake by Fullers earth bead at different temperatures

Initial concentration of cesium (mmol/L)	Liquid phase concentration of cesium at equilibrium (C_e, mmol/L)	Uptake by the adsorbent at equilibrium (Q, mmol/g)	K_d (mL/g)	Data correlation by: Langmuir parameters: b (mmol)	Langmuir parameters: Q_0 (mmol/g)	Langmuir parameters: Absolute error (%)	Langmuir parameters: Maximum positive error (%)	Langmuir parameters: Maximum negative error (%)	Freundlich parameters: K	Freundlich parameters: 1/n	Freundlich parameters: Absolute error (%)	Freundlich parameters: Maximum positive error (%)	Freundlich parameters: Maximum negative error (%)
293K													
0.414	0.323	0.0361	111.63	3.45×10^{-5}	0.229	3.77	5	5.2	0.077	0.5322	10.9	11.2	16.8
0.827	0.654	0.0692	105.75										
2.105	1.812	0.1173	64.73										
3.985	3.571	0.1654	46.32										
7.368	6.902	0.1865	27.02										
303K													
0.414	0.323	0.0361	111.63	4.16×10^{-5}	0.198	3.86	3.35	8.3	0.074	0.5004	12.96	16.9	18.1
0.752	0.602	0.0602	100										
1.654	1.391	0.1053	75.68										
3.834	3.421	0.1504	48.35										
7.368	6.955	0.1654	23.78										
313K													
0.414	0.323	0.0361	111.63	5.07×10^{-5}	0.177	5.00	6.05	10.4	0.073	0.468	14.04	18.3	19.7
0.752	0.602	0.0602	100										
1.654	1.395	0.1038	74.39										
3.834	3.477	0.1428	41.08										
7.368	6.992	0.1503	21.51										

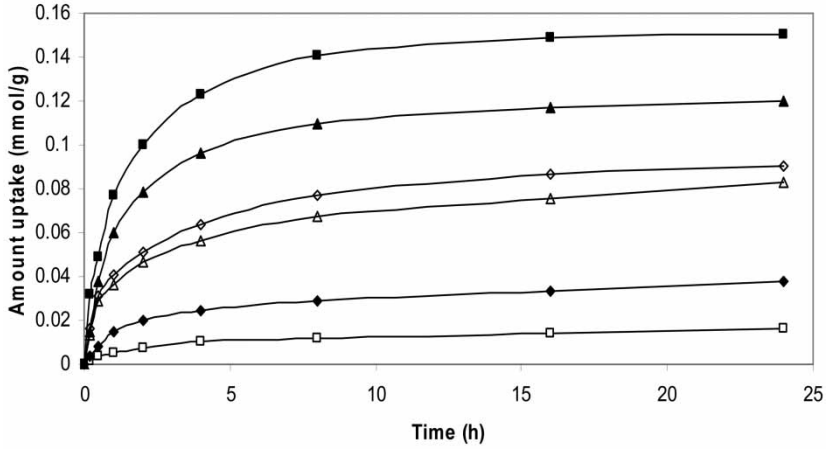

Figure 7. Effect of time and concentration on cesium removal by Fullers earth bead. The initial concentrations of the solution were (■) 7.52 mmol/L, (▲) 3.76 mmol/L, (◆) 1.5 mmol/L, (△) 0.752 mmol/L, (◆) 0.376 mmol/L, and (□) 0.075 mmol/L, respectively.

increased from 0 to 1 mol/L keeping strontium concentration same, the amount of cesium uptake decreased by almost 62%. This suggests that either the waste stream needs to be diluted or Na^+ should be removed prior to treatment by Fullers earth beads.

Effect of Temperature on Cesium Uptake by Fullers Earth Beads

The adsorption isotherms obtained at various temperatures were used to gain a better understanding of the adsorption mechanism. From the variation of K_d with temperature, the integral heat of adsorption can be calculated from the van't Hoff's equation.

$$\ln K_d = \frac{\Delta S^o}{R} - \frac{\Delta H^o}{RT} \quad \text{or} \quad \frac{\delta \ln K_d}{\delta T} = \frac{\Delta H^o}{RT^2} \tag{2}$$

The slope of a plot of ln K_d vs $1/T$ provides the value of ΔH° which was -3.627 kcal/mol suggesting exothermic nature of the adsorption process. The K_d values at different temperature is given in Table 4. An estimation of the variation in isosteric heat of adsorption with coverage can be calculated from the Calusius-Clapeyron equation.

$$\Delta H_{iso} = -R\left(\frac{\partial \ln C_e}{\partial(1/T)}\right)_q \tag{3}$$

The heat of adsorption at different loadings is shown in Fig. 8. The heat of adsorption of cesium decreased with the increase of loading that can be attributed to heterogeneity of the surface and multi-layer coverage. It is also evident from Fig. 8 that, as expected, the heat of adsorption approached the integral heat of adsorption at higher loading. This suggests that the surface became saturated with cesium and the heat of adsorption was approaching its equilibrium value.

Data Correlation

The Polanyi potential theory was modified to correlate the adsorption data at various temperatures and to check the consistency of the data. The Polanyi theory assumes that the adsorbent exerts long-range attractive forces on the gas or vapor surrounding it. These attractive forces generate a potential field which decreases as the distance between the gas and adsorbent surface increases. The theory has been used widely to correlate gas phase adsorption data. However, a number of researchers have extended the theory to the adsorption of solutes from the aqueous phase on to solid by expressing the potential in terms of saturation and equilibrium concentration. Wohleber and Manes (18) applied the modified theory of Hansen and Flacker (19) to correlate the adsorption data of totally miscible organic solutes in aqueous solution. Hasanian and Hines (20) correlated the adsorption data of butyric and hexanoic acid onto a macroreticular resin (XAD-2) with a limited success and concluded that the potential theory may not be applicable for such systems. However, no attempts were made to correlate adsorption data of metal ions from aqueous solution on a solid adsorbent. Hasany et al (21) used the Dubinin-Radushkevich (D-R) equation to correlate cadmium (II)

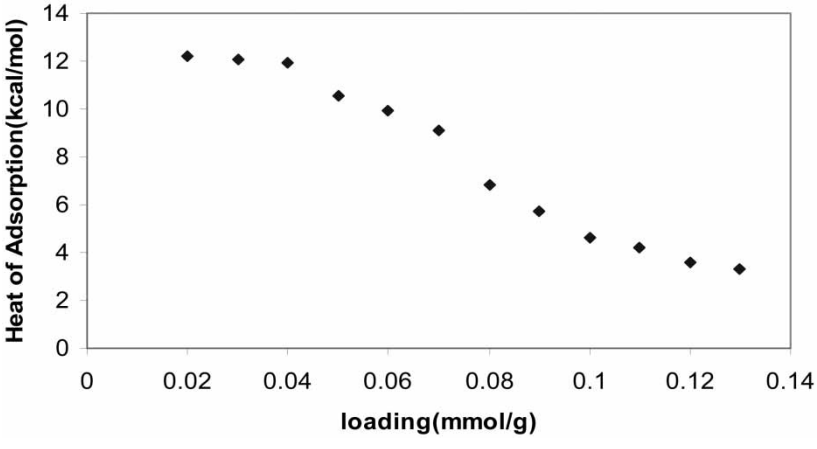

Figure 8. Isosteric heats of adsorption for cesium uptake on Fullers earth beads.

adsorption data on CdS. In order to apply the D-R equation, they calculated the potential using Polany's theory. A good fit to the data was reported. The adsorption potential (ε) for the cesium ion uptake was calculated from the following equation.

$$\varepsilon = RT \ln\left(\frac{a_s}{a}\right) \tag{4}$$

The activity was expressed in terms of mole fraction and activity coefficients ($a_s = x_s\gamma_s$). The activity coefficient of cesium ion in the solution was calculated using Davis equation given by Guibal et al. (22).

$$\log\gamma_i = -0.5109\left(\frac{\sqrt{I}}{I+\sqrt{I}} - 0.3I\right) \tag{5}$$

$$I = 0.5\sum_i C_i Z_i^2 \tag{6}$$

As can be seen from Fig. 9, an excellent fit to the data was obtained. A single characteristic curve was obtained for three temperatures as suggested by the Polanyi theory. Therefore, the equilibrium data can be calculated at various temperatures from the single characteristic equation.

Breakthrough Curve

Experimental breakthrough curves for cesium adsorption from a column packed with Fullers earth beads are shown in Fig. 10. Each run was continued for 15 hours using a Cs inlet concentration of 100 mg/L. The bed became saturated during this time period and breakthrough of cesium occurred after about 4 bed-volume. After 4 bed-volumes, the effluent concentration increased slowly and attained the inlet influent concentration at around

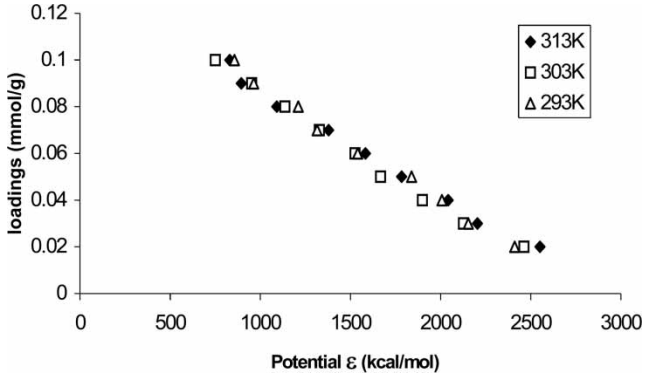

Figure 9. Characteristic curve for cesium uptake on Fullers earth beads.

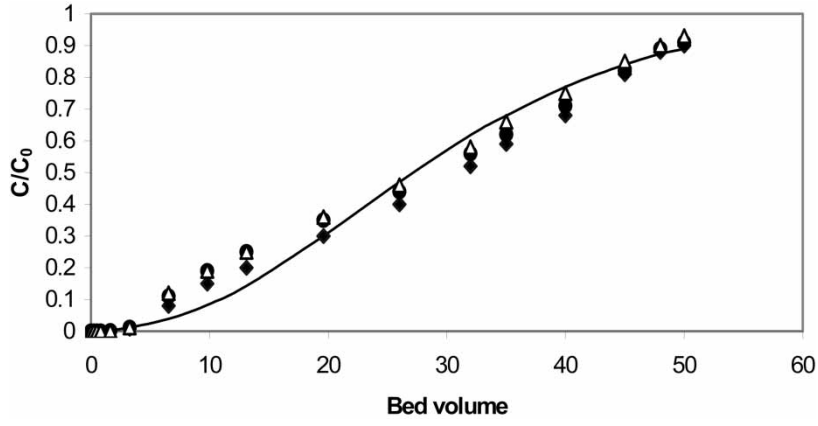

Figure 10. A comparison of experimental and theoretical breakthrough curves for cesium from a column packed with Fullers earth beads [(◆) 1st cycle, (●) 2nd cycle, (△) 3rd cycle, and solid line: theoretical curve]. (Column height: 12.7 cm; Inlet concentration: 0.746 mmol/L; Flow rate: 3.5 mL/min).

50 bed volumes. Although cesium broke through the column after 4 bed volume, by increasing the amount of adsorbent in the bed, the breakthrough time can be increased. The gradual increase of effluent concentration as shown in Fig. 10 with bed volumes, indicates slower adsorption kinetics.

Following an adsorption run, the bed was regenerated by passing NH_4Cl solution through the bed at a rate of 3.5 mL/min. Different concentrations of NH_4Cl solution were used to study the effect of NH_4Cl concentration and volume required for complete regeneration of the bed. Three adsorption and regeneration cycles were conducted using the same bed to check the degradation of the adsorbent due to repeated use. As can be seen from Fig. 10, no significant difference in the breakthrough characteristics was observed during the three adsorption cycles. A 0.01M of NH_4Cl was used to regenerate the column after first adsorption cycle. Approximately 6.0 bed volume was required to regenerate the column. In the second cycle, 1.5 bed volumes of 0.05M NH_4Cl solutions could regenerate the same column. The use of 0.1M NH_4Cl solution further reduced the amount and time for the regeneration of the same column. Figure 11 shows the concentration profile of cesium during regeneration in Cycle 1, 2 and 3.

Surface Kinetics

The beads contain about 68% of Fullers earth, which are active binding sites for cesium. Also SEM micrograph (Fig. 2) of beads exposed to cesium shows that the binding sites in the bead are distributed randomly. Therefore, a global approach for kinetic evaluation is more appropriate for this bead. For the case

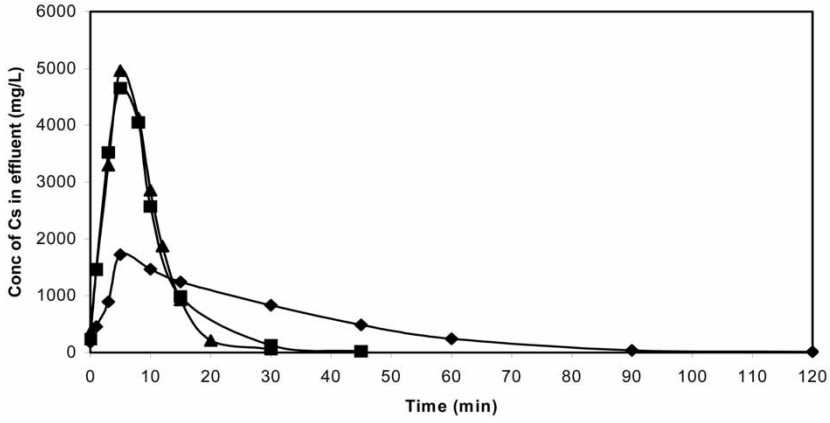

Figure 11. Regeneration of the column following adsorption of Cs by different concentration of NH_4Cl (◆) 0.01M NH_4Cl, (■) 0.05M NH_4Cl, and (▲) 0.1M NH_4Cl. (Flowrate of NH_4Cl: 3.5 mL/min).

in which a first-order reversible surface kinetic describes the change in solute concentration of the solid phase, the rate of uptake can be written as.

$$\left(\frac{\partial q_A}{\partial t}\right) = k_1 C_A - k_2 q_A = k_1\left(C_A - \frac{q_A}{K_d}\right) \quad [\mathrm{K}_d = k_1/k_2] \tag{7}$$

The mass balance equation for solute A based on the assumption that the resistance to the mass transfer is external, adsorption occurs onto the surface of the adsorbent, internal mass transfer occurs through the fluid phase which occupies the pores of the adsorbent, and internal mass transfer also occurs along the solid surfaces of the pores of the adsorbent, can be written as

$$-\frac{\varepsilon_p \nu}{1-\varepsilon_p}\left(\frac{\partial C_A}{\partial Z}\right)_t - \frac{\varepsilon_p}{1-\varepsilon_p}\left(\frac{\partial C_A}{\partial t}\right)_z = \left(\frac{\partial C_{AS}}{\partial t}\right)_z \tag{8}$$

The axial diffusion is neglected.

Introducing $\rho_s = \rho_b/(1-\varepsilon_P)$, and $q_A = C_{AS}/\rho_S$, and if the fluid content of the bed is small compared to the total volume of fluid throughput, then Equations (7) and (8) reduce to:

$$\frac{\partial Q}{\partial \tau} = X - Q \tag{9}$$

and

$$\frac{\partial X}{\partial \xi} = -X + Q \tag{10}$$

where,

$$\xi = \frac{k_1 \rho_b Z}{\varepsilon_p \nu} \quad \text{(bed length parameter)}$$

$$\tau = \frac{k_1}{K_d}\left(t - \frac{Z}{\nu}\right) \quad \text{(time parameter)}$$

$$X = \frac{C_A}{C_{A0}}$$

$$Q = \frac{q_A}{q_A^{\infty}}$$

The solution was given by Rosen (23) and was used to predict the breakthrough curves shown in Fig. 10. In the Rosen model, the kinetic parameters k_1 and k_2 were unknown. The values of k_1 and k_2 were determined by using a trial and error approach using Mathematica software. The best fit values for k_1 and k_2 were found to be 0.3694 min^{-1} and 12.79×10^{-3} min^{-1}, respectively which provided a correlation of the data within $\pm$ 5% of the experimental values. With these values of k_1 and k_2, the predicted breakthrough curve is shown in Fig. 10 along with the experimental data for all three adsorption cycles. As can be seen from the figure, an excellent fit to the experimental data was obtained with these values of k_1 and k_2. The values of k_1 and k_2 suggest that the forward rate, i.e., the adsorption process is much faster compared to the desorption rate.

CONCLUSION

Fullers earth based adsorbents were prepared using chitosan and sodium silicate as binder for adsorption of cesium in a dynamic column. However, the sodium silicate binder made the solution alkaline causing precipitation of cesium rather than physisorption. Therefore, Fullers earth beads prepared using chitosan beads were used for detailed evaluation for their capacity for cesium. Scanning electron micrographs showed that beads were porous. The equilibrium adsorption capacity of cesium was determined at different temperature using aqueous solution of CsCl of different concentrations and at different pH. The adsorption of cesium increased with the increase of pH of the aqueous solution up to a value of 6.5. The maximum adsorption capacity of cesium on chitosan coated Fullers earth beads at a pH of 6.5 and 30°C temperature could be about 26.3 mg/g of bead from a solution containing 1000 mg/L of CsCl as calculated from the Langmuir isotherm equation. Breakthrough data from a column was used to calculate the kinetic parameters of first-order reversible surface kinetic model. The best fit values for k_1 and k_2 for cesium adsorption on Fullers earth beads were found to be 0.3694 min^{-1} and 12.79×10^{-3} min^{-1}, respectively.

NOMENCLATURE

a_s	Activity of cesium ion at equilibrium concentration (mmol/L)
a	Activity of cesium at equilibrium at any concentration (mmol/L)
C_A	Concentration at the bed outlet, mmol/L
C_{A0}	Concentration of the inlet influent, mmol/L
C_{AS}	Concentration of the liquid phase at equilibrium, mmol/L
C_i	Initial concentration of cesium ion in solution, mg/L, or mmol/L
C_s	Equilibrium concentration of the cesium ion at saturation at a particular adsorption temperature (mmol/L),
C_e	Equilibrium concentration of cesium ion at equilibrium (mmol/L, or mg/L)
K_d	Distribution coefficient, mL/g
k_1	Kinetic parameter as defined in Equation 5, min^{-1}
k_2	Kinetic parameter as defined in Equation 5, min^{-1}
M	Mass of the adsorbent, g
Q_e	Amount adsorbed per unit mass of adsorbent, mg/g or mmol/g
q_A	Uptake of the solid phase, mg/g or mmol/g
q_A^{∞}	Uptake of the solid phase at saturation, mg/g or mmol/g
t	Time, min
v	Linear flow velocity (assumed constant), cm/sec
V	Volume, L
x	Mole fraction
Z	Distance from column entrance, cm
ΔS°	Entropy change for the process, $cal.deg.mol^{-1}$
ΔH°	Isoteric enthalpy change for the process, $cal.mol^{-1}$
R	Gas constant, cal. mol^{-1}. K^{-1}
T	Absolute temperature, K
ΔH_{iso}	Enthalpy change for the process, $cal.mol^{-1}$
I	Ionic strength, mol/L
Z_i	Ionic charge of component I in Equation 6
q	Uptake, mmol/g
ε_P	Bed porosity
ε	Adsorption potential ($kcal.mol^{-1}$),
ρ_s	Particle density, g/cm^3
ρ_b	Bed density, g/cm^3

REFERENCES

1. Behair, Sh.G., Benyamin, K., and Mekhail, F.M. (1998) Chemical precipitation of cesium from waste solutions with iron (II) hexacyanocobaltate (III) and triphenylcyanoborate. *Journal of Radioanalytical and Nuclear Chemistry*, 232 (1–2): 147–150.

2. Lateef, I.M., Huckman, M.E., and Anthony, R.G. (2000) Modelling cesium ion exchange on fixed bed columns of crystalline silicotitanate granules. *Ind. and Eng. Chem. Res.*, 39 (5): 1356–1363.
3. Gu, D., Nguyen, L., Philip, C.V., Huckman, M.E., and Anthony, R.G. (1997) Cs^+ ion exchange kinetics in complex electrolyte solutions using hydrous crystalline silicotitanates. *Ind. Eng. Chem. Res.*, 36: 5377–5383.
4. Pawaskar, C.S., Mohapatra, P.K., and Manchanda, V.K. (1999) Extraction of actinides fission products from salt solutions using polyethylene glycols (PEGs). *Journal of Radioanalytical and Nuclear Chemistry*, 242 (3): 627–634.
5. Dozol, J.F., Simon, N., Lamare, V., Rouquette, H., Eymard, S., Tournois, B., Marc, D., and Marcias, R.M. (1999) A solution for cesium removal from high salinity acidic or alkaline liquid waste: The crown calix[4]arenas. *Sep. Sci. Technol.*, 34 (6&7): 877–909.
6. Arena, G., Contino, A., Margi, A., Sciotto, D., Spoto, G., and Torrisi, A. (2000) Strategies based on calixcrowns for the detection and removal of cesium ions from alkali- containing solutions. *Ind. Eng. Chem. Res.*, 39: 3605–3610.
7. Zeng, Z., Philips, C.V., Anthony, R.G., Krumhansl, J.L., Trudell, D.E., and Miller, J.E. (1996) Ion exchange of group I metals by hydrous crystalline silicotitanates. *Ind. Eng. Chem. Res.*, 35 (11): 4246–4256.
8. Sing, I.J. and Misra, B.M. (1996) Studies on sorption of radiocesium on copper-hexacyanoferrate-loaded resins. *Separation Science and Technology*, 31 (12): 1695–1705.
9. Harjula, R., Lehto, J., Paajanen, A., and Brodkin, L. (2001) Removal of radioactive cesium from nuclear waste solutions with the transition metal hexacyanoferrate ion exchanger Cs-treat. *Nuclear Science and Engineering*, 137: 206–214.
10. Anthony, R.G., Dosch, R.G., Gu, D., and Philip, C.V. (1994) Use of silicotitanates for removing cesium and strontium from defense waste. *Industrial and Engineering Chemistry Research*, 33: 2702–2705.
11. Lee, D.D., Walker, J.F., Taylor, P.A., and Hendrickson, D.W. (1997) Cesium removal flow studies using ion exchange. *Environmental Progress*, 16 (4): 251–262.
12. Hasan, S. (2005) Development of materials for the removal of metal ions from radioactive and non-radioactive waste streams. Ph. D. Dissertation, University of Missouri-Columbia May 2005.
13. Hasan, S., Krshnaia, A., Ghosh, T.K., Viswanath, D.S., Boddu, V.M., and Smith, E.D. (2006) Adsorption of divalent cadmium (Cd (II)) on chitosan coated perlite. *Ind. Eng. Chem. Res.*, 45: 5066–5077.
14. Hasan, S., Krshnaia, A., Ghosh, T.K., Viswanath, D.S., Boddu, V.M., and Smith, E.D. (2003) Adsorption of chromium (VI) on chitosan coated perlite. *Sep. Sci. Technol.*, 38 (15): 3775–3793.
15. Goldstein, J.I., Newbury, D.E., Echlin, P., Joy, D.C., Romig, A.D., Lymand, C.E., Fiori, C., and Lifshin, E. (1992) Scanning electron microscopy and X-ray microanalysis. Plenum Press: New York.
16. Teterin, Y.A., Nefedov, V.I., Ronneau, C., Vanbegin, J., Cara, J., Utkin, I.O., Teferin, A.Y., Nikitin, A.S., Ivanov, K.E., Vukcevic, L., and Bek-Uzarov, G. (2001) X-ray photoelectron spectroscopic study of U and Cs containing hot particles prepared under laboratory conditions. Accounting for parameters of U 5f, U 4f, and Cs 3d, Cs 4d electron lines. *Radiochemistry*, 43 (6): 604–609.
17. Kaminski, W. and Modrzejewska, Z. (1997) Equilibrium studies for the sorption of metal ions onto chitosan. *Sep. Sci. Technol.*, 32 (16): 2659–2668.

18. Hansen, R.S. and Fackler, W.V. (1953) A generalization of the Polanyi theory of adsorption from solution. *J. Phys. Chem.*, 57: 634–637.
19. Wohleber, D.A. and Manes, M. (1971) Application of the Polanyi adsorption theory to adsorption from solution on activated carbon. III. Adsorption of miscible organic liquids from water solution. *J. Phys. Chem.*, 75: 3720–3723.
20. Hasanain, M.A. and Hines, A.L. (1981) Application of the adsorption potential theory to adsorption of carboxylic acids from aqueous solutions onto a macroreticular resin. *Ind. Eng. Chem. Process. Dev.*, 20: 621–625.
21. Hasany, S.M., Saeed, M.M., and Ahmed, M. (1998) Uptake of cadmium(II) ions by cadmium sulphide from aqueous solutions. *Radiochim. Acta.*, 83: 205–210.
22. Guibal, E., Milot, C., and Roussy, J. (2000) Influence of hydrolysis mechanisms on molybdate sorption isotherms using chitosan. *Sep. Sci. Technol.*, 35 (7): 1021–1038.
23. Rosen, J.B. (1954) General numerical solution for solid diffusion in fixed beds. *Industrial and Engineering Chemistry*, 46 (8): 1590–1594.
24. DePaoli, S.M. and Perona, J.J. (1996) Model for Sr-Cs-Ca-Mg-Na ion exchange uptake kinetics on chabazite. *AIChE Journal*, 42 (12): 3434–3441.
25. Behrens, E.A., Sylvester, P., and Clearfield, A. (1998) Assessment of a sodium nonatitanate and pharmacosiderite type ion exchangers for strontium and cesium removal from DOE waste simulants. *Environmental Science and Technology*, 32: 101–107.
26. Apak, R., Atun, G., Guclu, K., Tutem, E., and Keskin, G. (1995) Sorptive removal of cesium-137 and strontium-90 from water by unconventional sorbents. II Usage of bauxite wastes (Red mud). *Journal of Nuclear Science and Technology*, 32 (10): 1008–1017.
27. Tsai, S.-H., Ouyang, S., and Hsu, C.-M. (2001) Sorption and diffusion behavior of Cs and Sr on Jih-Hsing bentonite. *Applied Radiation and Isotopes.*, 54: 209–215.
28. Bostic, D.T., Arnold, W.D., Guo, B., and Burgess, M.W. (1997) The evaluation of sodium modified chabazite zeolite and resorcinol-formaldehyde resin for the treatment of contaminated process wastewater. *Separation Science and Technol*, 32 (1–4): 793–811.
29. Sylvester, P. and Clearfield, A. (1995) The extraction of 137Cs and ^{89}Sr from waste simulants using pillard montomorillonite. *Separation Science and Technol*, 32 (5): 425–429.
30. Samantha, S.K., Theyvunni, T.K., and Misra, B.M. (1998) Column behavior of resourcinol-formaldehyde polycondensate resin for radiocesium removal from simulated radwaste solution. *J. Nuc. Sci. Technol.*, 33 (11): 1605–1615.